Journal of Crystal Growth 531 (2020) 125334

Contents lists available at ScienceDirect

Journal of Crystal Growth

journal homepage: www.elsevier.com/locate/jcrysgro

Numerical analysis of effect of thermal stress depending on pulling rate on behavior of intrinsic point defects in large-diameter Si crystal grown by Czochralski method

Yuji Mukaiyama[a,*], Koji Sueoka[d], Susumu Maeda[c], Masaya Iizuka[a], Vasif M. Mamedov[b]

[a] STR Japan K.K., East Tower 15F, Yokohama Business Park, 134, Goudo-cho, Hodogaya-ku, Yokohama, Kanagawa 240-0005, Japan
[b] STR Group—Soft-Impact, Ltd., Bolshoi Sampsonievskii pr. 64, Build. "E", 194044 St. Petersburg, Russia
[c] GlobalWafers Japan Co., Ltd., 6-861-5 Higashiko, Seiro, Niigata 957-0197, Japan
[d] Okayama Prefectural University, 111 Kuboki, Soja, Okayama 719-1197, Japan

ARTICLE INFO

Communicated by P. Rudolph

Keywords:
A1. Computer simulation
A1. Point defects
A1. Stresses
A2. Czochralski method
B2. Semiconducting silicon

ABSTRACT

We analyzed the effects of thermal stress and pulling rate on the behavior of intrinsic point defects in a silicon (Si) single crystal grown by the Czochralski (Cz) method using a numerical approach. The thermal equilibrium concentration of the intrinsic point defects (vacancy, *V*, and self-interstitial Si atom, *I*) was simulated as a function of thermal stress, which was obtained via *ab -initio* calculations. Furthermore, the point defect dynamics in the crystal were solved within a framework of a two-dimensional (2D) axisymmetric steady-state global heat and mass transport model of Si crystal growth by the Cz method. The numerical simulations revealed that both magnitude and distribution of the thermal stress depend on the pulling rate. Moreover, they impact the formation and distribution of intrinsic point defects in a growing Si single crystal.

1. Introduction

Silicon (Si) single crystals have been industrially produced by the Czochralski (Cz) method and used as substrate material for electrical devices like LSI and power MOSFETs. For such devices, a precise control of the intrinsic point defects (vacancy (*V*) and self-interstitial Si atom (*I*)) and grown-in defects (voids and dislocation clusters) is required to improve and optimize device performance. During the last few decades, several theoretical and numerical models of the behavior of intrinsic point defects in a Si single crystal grown by the Cz method have been proposed and used for the optimization of intrinsic point defect distribution [1,2]. Recently, the effects of thermal stress in a growing Si crystal on the behavior of intrinsic point defects have been determined by a theoretical approach [3,4]. Previous researchers compared experimental data and simulations of the effect of thermal stress in Si crystals (diameters of ~300 mm) grown by the Cz method. They showed that a compressive stress of ~20 MPa enhances the incorporation of *V* into a growing crystal [5,6]. It is well known that growth condition and crystal size are strongly associated with the introduction of a thermal stress to the growing crystal [7–9]. In particular, the crystal pulling rate is one of the most fundamental factors governing both thermal stress and the incorporation of intrinsic point defects. Therefore, studying the relationship between the pulling rate, thermal stress, and point defects is of great interest for the optimization of Si crystal quality in the Cz growth process. However, detailed studies on this topic are lacking. Recently, we constructed a theoretical model of the thermal equilibrium concentration of intrinsic point defects as a function of thermal stresses in a growing Cz-Si crystal [10]. The developed model was implemented to the commercial crystal growth simulator *CGSim* package of the STR Group, Inc. [11]. Here, we present steady-state simulation results solved with a two-dimensional (2D) axisymmetric model of the Cz Si growth (large diameters of 400 mm) and discuss the effects of thermal stress with respect to the pulling rate on the distributions of the *V* and *I* concentrations in a growing Si crystal.

2. Mathematical models

2D axisymmetric steady-state simulations were performed with the Basic module of the *CGSim* software package for computations of the global heat and mass transfer in the entire furnace, taking into account the turbulent convection in the melt and gas regions, the thermal stress, and dynamics of intrinsic point defects in the crystal. The series of mathematical models used in the simulation are described in this

* Corresponding author.
E-mail address: yuji.mukaiyama@str-soft.co.jp (Y. Mukaiyama).

https://doi.org/10.1016/j.jcrysgro.2019.125334
Received 21 August 2019; Received in revised form 30 October 2019; Accepted 31 October 2019
Available online 02 November 2019
0022-0248/

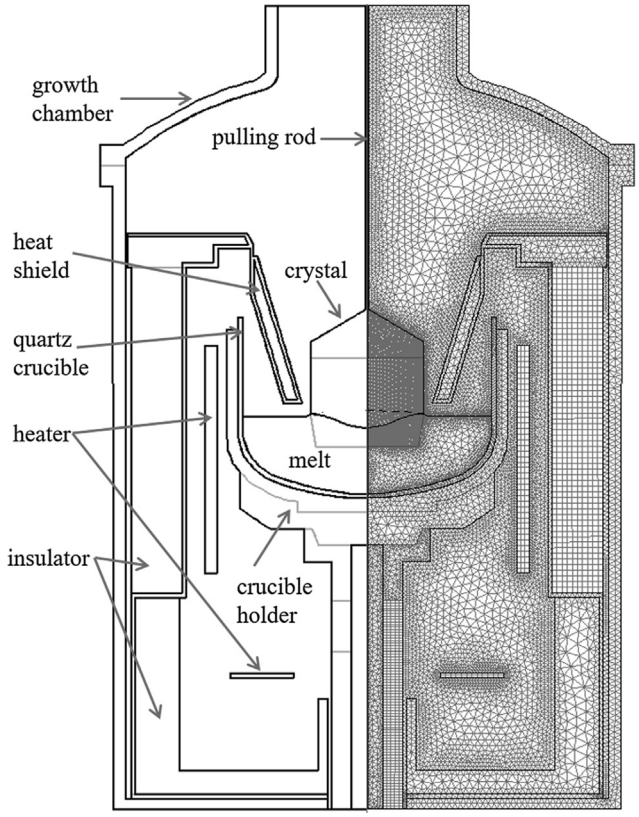

Fig.1. Material arrangement (left) and computational grids (right) in a furnace.

section.

2.1. Global heat, mass transport and thermal stress

The governing differential equations for the momentum, heat transfer (conduction, convection, and radiation), and mass transfer in a computational domain are solved self-consistently [12].

The turbulent mixing of the flow (gas and melt domain) is described within the Reynolds-Averaged Navier-Stokes equation approach. The one-equation model is used to determine turbulent viscosity in the melt and gas region [13]. As boundary conditions along the free melt surface, the momentum exchange between the gas and the melt flow and the Marangoni condition must be satisfied for a tangential velocity component.

In the iterative computation process, the crystal/melt interface is corrected according to the Stefan problem. The thermal stress in the crystal is explicitly calculated based on the calculated temperature distribution. For this purpose, all constraining conditions at the crystal side surface and crystal/melt and seed/crystal interfaces are assumed to be free. The respective equations are solved with a solver based on the finite-volume method. The computational grid for the Cz furnace is shown in Fig. 1. The material properties of the Si crystal and melt used in the simulations are described in [12]. Moreover, the power of the side heater is controlled by the proportional-integral-differential (PID) algorithm to achieve the target crystal pulling rate.

2.2. Thermal equilibrium concentration of vacancies (V) and self-interstitial Si atoms (I)

The thermal equilibrium concentrations of *V* and *I* are represented as a function of the thermal stress in a growing Si crystal. The functions and parameter sets for *V* and *I* are referred from [10]. In the function, the isotropic thermal stress is defined as the mean stress: $\sigma_{mean} = (\sigma_{11} + \sigma_{22} + \sigma_{33})/3$. The calculated thermal stress of the global heat transfer is explicitly used for the calculation of the thermal equilibrium concentration of the intrinsic point defects. Moreover, the thermal

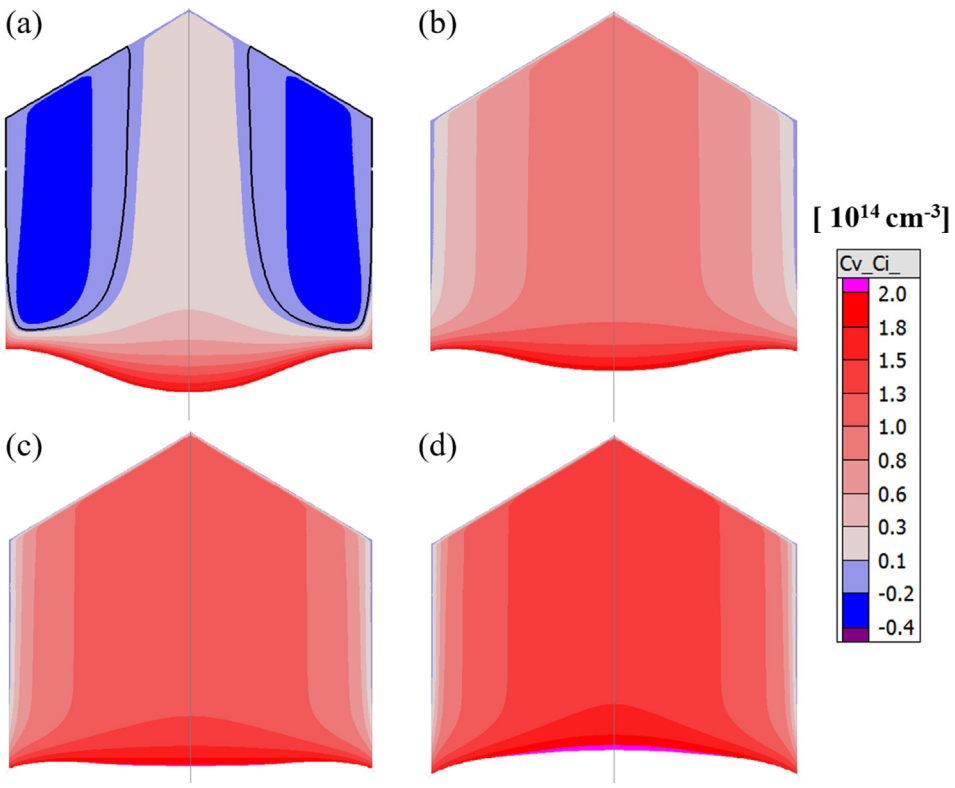

Fig.2. C_v-C_i distribution in crystal for pulling rates of 0.2 (a), 0.4 (b), 0.6 (c), and 0.8 mm/min (d). The black contours represent C_v-C_i = 0. The magenta regions represent regions with higher values than 2.0 (10^{14} cm^{-3}). (For interpretation of the references to colour in this figure legend, the reader is referred to the web version of this article.)

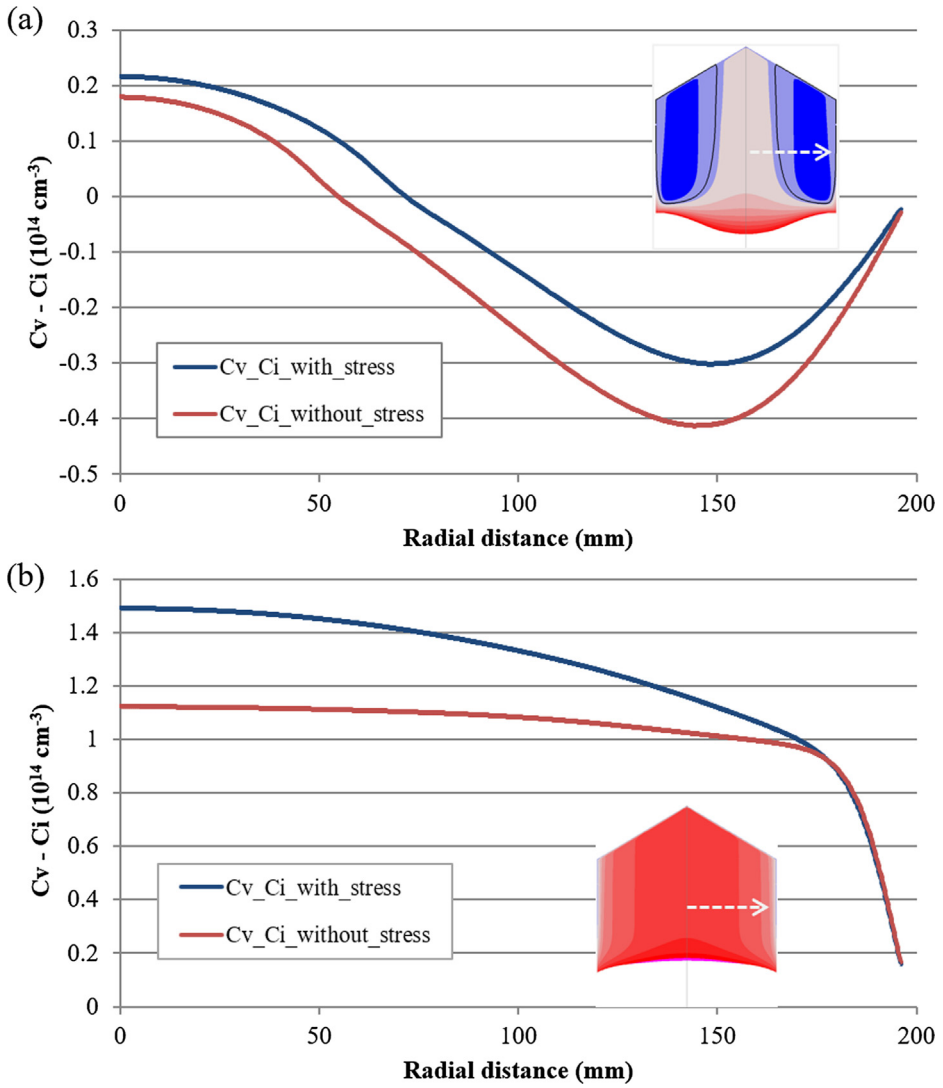

Fig.3. C_v-C_i distribution along radial direction in crystal for pulling rates of 0.2 (a) and 0.8 mm/min (b).

stress near the crystallization front is rather approximately planar and not isotropic. Therefore, the concentrations of V and I are corrected concentrations under planar stress with correction parameters [10]. Furthermore, the effect of the incorporated oxygen impurities on the V formation is additionally considered [10]. Oxygen of a certain concentration (approximately $10^{18}\,cm^{-3}$) is always incorporated in a growing Si crystal. However, its impact is weak and only slightly increases the V concentration [10]. The functions of the thermal equilibrium concentration are specified for the crystal/melt interface and crystal side surface as boundary conditions for the point defect transport simulations described below. The simulation model considering the thermal stress effect was validated with experiment of a 300 mm diameter Si crystal growth by the Cz method, and the simulation result agreed well with the experimental data [6].

2.3. Point defect transport in growing Si crystal

In this study, a 2D axisymmetric model was applied for the V and I dynamics to predict the distribution of the point defect concentration in a growing Si crystal. This model includes the point defect formation at the crystallization front and the subsequent incorporation into the crystal by advection based on the pulling rate, diffusive transport, and recombination inside the crystal bulk. The steady-state governing equations for the point defect dynamics in a growing crystal are as follows:

$$V_p \cdot \nabla C_k = \nabla \cdot (D_k \nabla C_k) + 4\pi a_r (D_V + D_I) \times \exp\left(\frac{-\Delta G}{k_B T}\right)(C_{Ie} C_{Ve} - C_I C_V) \quad (1)$$

$$D_k = D_{k,0} \times \exp\left(\frac{-\Delta G_{Dk}}{k_B T}\right) \quad (2)$$

Here, k denotes V or I; C_k and D_k are the concentration and diffusion coefficients of the point defects, respectively. The pre-exponential factor $D_{k,0}$ and activation energy ΔG_{Dk} have been proposed in [14,15]. Furthermore, local diffusivity depends on the local crystal temperature obtained through the global heat and mass transfer simulations. The equilibrium concentrations C_{Ie} and C_{Ve} are the functions of the local temperature and thermal stress (see Section 2-2). In the advection term of Eq. (1), V_p represents the specified pulling rate. The last term in Eq. (1) represents the recombination rate, which depends on the local temperature, capture radius a_r, and free energy barrier of the recombination (ΔG) [10].

3. Results and discussion

A schematic of the Cz furnace and its components used for the numerical simulations are shown in Fig. 1. The furnace geometry and

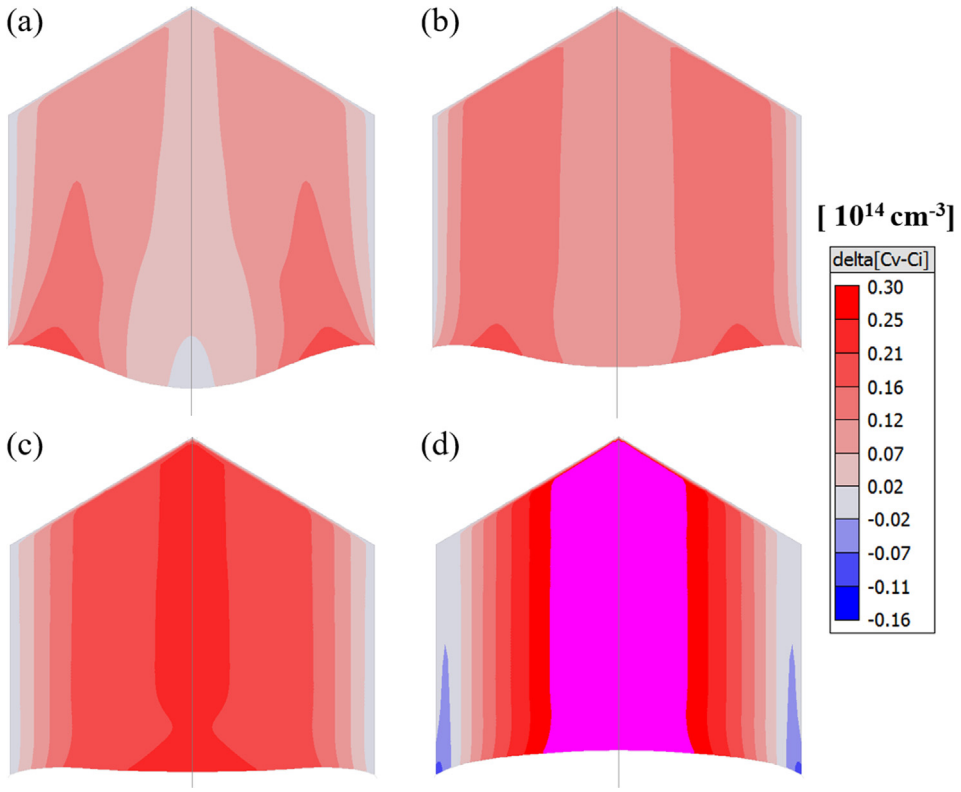

Fig.4. Excess defect concentration ($\Delta(C_v\text{-}C_i)$) distribution in crystal for pulling rates of 0.2 (a), 0.4 (b), 0.6 (c), and 0.8 mm/min (d). Magenta represents regions with higher values than 0.3 (10^{14} cm^{-3}). (For interpretation of the references to colour in this figure legend, the reader is referred to the web version of this article.)

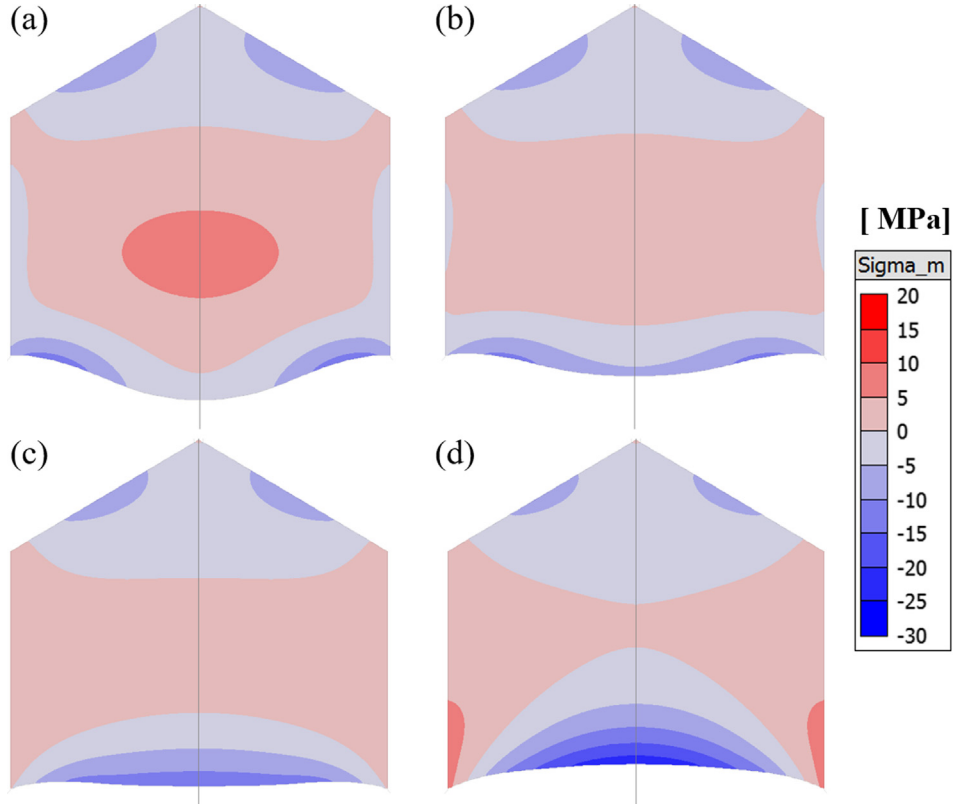

Fig.5. Thermal stress (mean stress) distribution in crystal for pulling rates of 0.2 (a), 0.4 (b), 0.6 (c), and 0.8 mm/min (d).

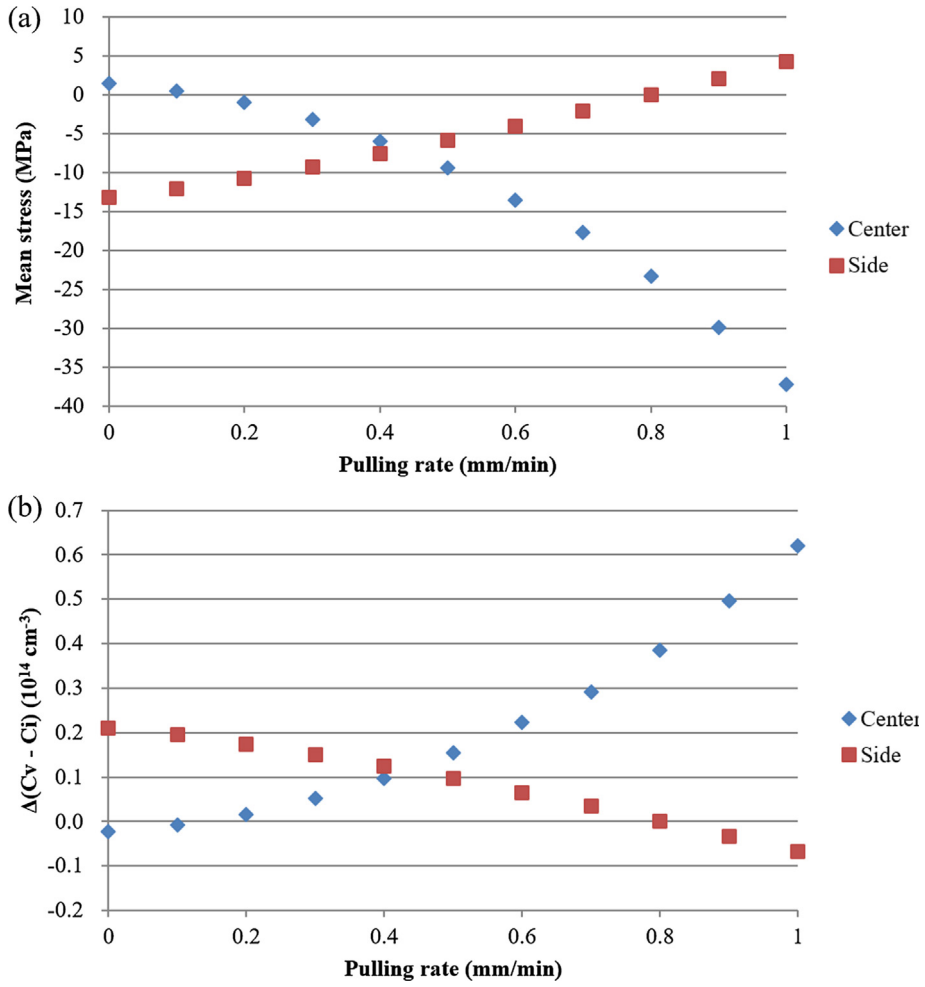

Fig.6. Thermal stress (mean stress) (a) and excess defect ($\Delta(C_v\text{-}C_i)$) concentration (b) as functions of the pulling rate.

basic process conditions for the Cz Si growth were proposed in [16]. Moreover, the reactor pressure was maintained at 1000 Pa with an argon gas flow. The diameter and height of the crystal were 400 mm and 364 mm, respectively.

The rotation speeds of the crucible and crystal were 8 rpm and 13 rpm with opposite rotation directions, respectively. The numerical simulations were performed with different pulling rates while the other growth conditions remained constant. In this section, the numerical simulation results are presented, and the effects of thermal stress with respect to the crystal pulling rate on the behavior of the intrinsic point defects in a Si crystal growing by the Cz method are discussed.

Fig. 2 shows the C_v-C_i distribution calculated considering the effect of the thermal stress in the crystal with the corrected interface shape for various pulling rates. The value of C_v-C_i represents the difference between the *V* and *I* concentrations, which determines the dominant defect in the crystal. As shown in Fig. 2(a), both *V*- and *I*- rich regions occur in the crystal for the lowest pulling rate (0.2 mm/min). With increasing pulling rate, C_v-C_i increases, and the *V*- rich region becomes dominant in the entire crystal area (Fig. 2(b)–(d)). The dependency on the pulling rate is a general phenomenon that has been well studied. To investigate the effect of the thermal stress, the C_v-C_i distribution was compared for cases with and without stress effect. Fig. 3(a) presents the C_v-C_i distribution in radial direction for a pulling rate of 0.2 mm/min. The C_v-C_i values with stress effect are higher than those without stress across the entire region. The difference is particularly remarkable in the side region. In addition, Fig. 3(b) illustrates the distributions for a high pulling rate (0.8 mm/min). Interestingly, the difference in the center region is higher than in the side region, unlike that of 0.2 mm/min case.

To clearly illustrate the impact of the thermal stress on the formation of point defects and their distribution in the crystal, we present the difference between the C_v-C_i values with and without stress effect ($\Delta(C_v - C_i) = (C_v - C_i)_{with\_stress} - (C_v - C_i)_{without\_stress}$) as a function of the pulling rate in Fig. 4. We call this value "the excess defect". A positive value implies that the excess *V* concentration is promoted by a thermal compressive stress. The position of the maximal excess *V* concentration in the growth interface shifts from the side region to the center region with increasing pulling rate. The shift to another region indicates that the region in which the thermal stress promotes a maximal excess *V* formation is changed according to the pulling rate. Furthermore, the excess *V* moves to the inside of the grown crystal and increase the concentration of *V*. To study the pulling rate dependency of excess *V* formation, we analyzed the impact of the pulling rate on thermal stress in a growing crystal. Fig. 5 shows the mean stress σ_{mean} distribution in the grown crystal for various pulling rates. The positive and negative values indicate tensile and compressive stresses, respectively. Evidently, the maximal compressive stress along the growth interface shifts from the side region to the center region. In addition, the maximum increases with increasing pulling rate. We assume that the change in the crystallization interface is the reason for the shifting maximal stress. It is well known that the thermal stress in a growing crystal is related to the growth interface shape, which is related to the pulling rate. For an approximately planar shape, a lower radial temperature gradient can be provided near the interface, which leads to a lower compressive or tensile stress near the crystallization interface. For an approximately concave shape, a higher radial temperature gradient and higher compressive stress can be formed. In our results, the

interface shape at the center region drastically changes from convex to concave, and the compressive stress increases with increasing pulling rate. The interface shape of the side region remains slightly concave for all pulling rates. To investigate the relationship between the pulling rate, thermal stress, and excess defects due to thermal stress along the interface in detail, thermal stress and excess defect concentration in the center and side regions are plotted as functions of the pulling rate in Fig. 6(a) and (b) (23 mm distance from the crystal side surface near the interface), respectively. According to the results, the stress changes and excess defect concentration exhibit a significant positive correlation. In Fig. 6(a), the compressive stress at the center position sharply increases with increasing pulling rate. The compressive stress at the side position bluntly decreases and finally converts to tensile stress. According to Fig. 6(b), the excess *V* concentration changes according to the increase in the pulling rate. Moreover, the excess *V* concentrations at the center and side positions increase and decrease, respectively. For the highest pulling rate (1.0 mm/min), the maximal compressive stress and excess *V* concentration occur at the center position. Furthermore, in Fig. 6 (b), slightly negative values of $\Delta(C_v\text{-}C_i)$ ($-7 \times 10^{11}\,cm^{-3}$ – ($-7 \times 10^{12}\,cm^{-3}$)) occur at the center position for lower pulling rates and at the side position for higher pulling rates. The negative value in Fig. 6(b) is due to the tensile stress corresponding to the positive value of thermal stress (1–4 MPa) in Fig. 6(a). It has been proposed in previous literature [17] that tensile stress impacts the formation enthalpy and slightly strengthens the *I* formation. Thus, it is assumed that this negative value regards an excess *I* rather than an excess *V* concentration. However, these values are very small and might not significantly contribute to the distribution of point defects in the crystal.

According to these results, we found that the *V* formation and intrinsic point defects distribution in a Si crystal grown by the Cz method strongly depend on the interface shape with respect to pulling rate via thermal stress. Nakamura et al. [5,18] and Sueoka et al. [4] have proposed that high compressive stress changes the critical V/G ratio, where V is the pulling rate and G is the axial temperature gradient at the crystal/melt interface, which determines the type of the intrinsic point defects in the crystal. Suggested simulation model based on the global heat transfer directly describes the effect of thermal stress for the behavior of *V* and *I* in the growing Si crystal. Therefore, we think our findings provides a deeper insight to find the optimized growth conditions for growing of defect-free Si crystal under high thermal stress. In particular, the described simulation model is useful for pulling rate optimization to improve the crystal quality and production cost of forthcoming production of large Si ingot.

4. Conclusion

A function for the thermal equilibrium concentration with respect to thermal stress was implemented in the crystal growth simulation software *CGSim* package. We studied the effects of thermal stress for various pulling rates on the behavior of intrinsic point defects in a single Si crystal growing by the Cz method using a numerical approach. The results reveal that the changes in stress and point defect concentration in the growing crystal, which depend on the interface shape, exhibit a good correlation. This study provides essential insight into the behaviour of point defects and the optimization of the growth conditions for Si single crystals with the Cz method; in particular, for large ingots with high thermal stress. Nevertheless, it should be noted that there are many factors affecting the thermal stress in the growing Si crystal by the Cz method, such as a crystal rotation speed and design of hot zone etc. Therefore, their effects on thermal stress and intrinsic point defects should be investigated in the future.

Declaration of Competing Interest

Author declares that there is no conflicts of interest.

Acknowledgement

This work is partially supported by the JSPS KAKENHI (grant numbers 25390069 and 16K04950) and the Foundation for Assistance to Small Innovative Enterprises (FASIE, Russia) within the ERA.Net RUS Plus Project (grant number 295ГР/21031).

References

[1] V.V. Voronkov, R. Falster, J. Appl. Phys 86 (1999) 5975.
[2] T. Sinno, Electrochem. Soc. Proc. PV2002-2 (2002) 212–223.
[3] J. Vanhellemont, J. Appl. Phys 110 (2011) 063519.
[4] K. Sueoka, E. Kamiyama, J. Vanhellemont, J. Crystal Growth 363 (2013) 97.
[5] Kozo Nakamura, Ryota Suewaka, Bonggyun Ko, ECS Solid State Lett. 3 (3) (2014) N5–N7.
[6] Eiji Kamiyama, Yoshiaki Abe, Hironori Banba, Hiroyuki Saito, Susumu Maeda, Alexander Kuliev, Masaya Iizuka, Yuji Mukaiyama, Koji Sueokad, ECS J. Solid State Sci. Technol. 5 (10) (2016) P553–P555.
[7] G.A.O. Yu, T.U. Hailing, W.O.U. Qigang, D.A.I. Xiaolin, X.I.A.O. Qinghua, Rare Metals 26 (6) (2007) 607.
[8] Y.F. Zou, H. Zhang, V. Prasad, J. Crystal Growth 166 (2013) 476–482.
[9] K. Takano, Y. Shiraishi, J. Matsubara, T. Iida, N. Takase, N. Machida, M. Kuramoto, H. Yamagishi, J. Crystal Growth 229 (2001) 26–30.
[10] Koji Sueoka, Yuji Mukaiyama, Susumu Maeda, Masaya Iizuka, Vasif M. Mamedov, ECS J. Solid State Sci. Technol. 8 (4) (2019) P228–P238.
[11] http://www.str-soft.com/products/CGSim/.
[12] V.V. Kalaev, D.P. Lukanin, V.A. Zabelin, Yu.N. Makarov, J. Virbulis, E. Dornberger, W. von Ammon, Mater. Sci. Semicond. Process. 5 (2003) 369–373.
[13] M. Wolfshtein, Int. J. Heat Mass Transf. 12 (12) (1969) 301.
[14] K. Sueoka, E. Kamiyama, J. Vanhellemont, J. Appl. Phys. 114 (2013) 153510.
[15] K. Nakamura, T. Saishoji, J. Tomioka, Semiconductor Silicon 2002, PV 2002-2, The Electrochemical Society Proceedings Series, 2002, p. 554.
[16] Y. Shiraishi, K. Takano, J. Matsubara, T. Iida, N. Takase, N. Machida, M. Kuramoto, H. Yamagishi, J. Crystal Growth 17 (2001) 229.
[17] K. Sueoka, K. Nakamura, J. Vanhellemont, J. Crystal Growth 474 (2017) 89–95.
[18] Kozo Nakamura, Proceeding of The 8th Forum on the Secience and Technology of Silicon Material 2018(Okayama) No. 18-21, 2018, Okayama, Japan.